International Journal of Thin Films Science and Technology

http://dx.doi.org/10.18576/ijtfst/150103

Single-Cycle Growth of GaAs-Ge-GaAs Heterostructures from Bismuth Melt: Structural and Photoelectronic Properties

A.Sh.Razzokov[1], V.V.Girzhon[2], A.S.Saidov[3], O.V.Smolyakov[2], A.V.Dolbin[4], P.V.Mateychenko[4] and D. E. Koshchanova[1,]*

[1] Urgench State University, 14 Kh.Alimdjan, Urgench, 220100, Uzbekistan
[2] National University "Zaporizhzhia Polytechnic", 64 Zhukovsky Str., Zaporizhzhia, 69063, Ukraine
[3] Physical-Technical Institute NPO "Physics-Sun of the Academy of Sciences of the Republic of Uzbekistan, 2B, Ch. Aitmatov St., Tashkent, 100084, Uzbekistan
[4] B.Verkin Institute for Low Temperature Physics & Engineering, National Academy of Sciences of Ukraine. 47 Nauky Ave., Kharkiv, 61103, Ukraine

Received: 12 Jul. 2025, Revised: 22 Sep. 2025, Accepted: 7 Nov. 2025
Published online: 1 Jan. 2026

Abstract: In this work, the possibility of forming a substitutional solid solution of the $(Ge_2)_{1-x}(GaAs)_x$ type was demonstrated through calculations of the generalized atomic moment. In a single technological cycle, GaAs-Ge-$(Ge_2)_{1-x}(GaAs)_x$ ($0 \le x \le 1$) heterostructures were obtained from a limited bismuth-based melt solution on single-crystal GaAs (100) substrates. The $(Ge_2)_{1-x}(GaAs)_x$ film with a variable chemical composition allowed to expand the spectral range of the photosensitivity of the nGaAs-pGe-p$(Ge_2)_{1-x}(GaAs)_x$ structure (0.65 - 2.0 eV). A method has been developed for producing highly crystalline solid solutions with a variable chemical composition (the dislocation density on the films surface was $2 \cdot 10^4$ cm^{-2}, the surface roughness varied within the range of 1.18 - 1.66 nm).

Keywords: surface, epitaxial layer, heterostructure, solid solution.

1 Introduction

The fabrication of highly crystalline heterostructures as semiconductor multilayer epitaxial films for the photodetector's development (in particular in the IR spectrum) and photoconverters was an urgent task [1, 2]. The development and manufacture of solar panels, p-channel transistors, and mixing diodes also require new materials with a wider range of performance characteristics. In addition, photodetectors based on GaAs/Ge/GaAs heterostructures are of considerable interest in such promising areas as nonlinear conversion of optical frequencies, production of topological insulators, solid-state lasers operating in the IR region, etc. [3, 4].

There are quite a lot of studies in the scientific literature devoted to the production of such heterostructures. Thus, in [5], using molecular beam epitaxy (MBE), GaAs/Ge/GaAs heterostructures were obtained on GaAs (100) substrates with high quality (110) and (111) interfaces, having a uniform morphology and a roughness about 0.2–0.3 nm. In [6], using the same method, similar heterostructures were obtained on a GaAs (113) substrate, and in [7] a new method for the implementation of such heterostructures was provided. Using the MBE method, the authors [8] managed to obtain cascade structures GeSn/Ge/GaAs and GeSn/Ge/AlAs/GaAs on GaAs (100) substrates using two different buffer layers consisting of Ge/GaAs and Ge/AlAs for near- and mid-field infrared range technologies of highly efficient photodetectors and laser devices. However, this acquisition process turned out to be quite complex and expensive [9,10].

In [11, 12], epitaxial films $(GaAs)_{1-x}(Ge_2)_x$ were grown on GaAs (100) and GaAs (111) substrates using planar magnetron sputtering without excess As pressure. It has been shown that the transition between the crystal structures of zinc blende and diamond occurs at $x \approx 0.35$. Here, Ga and As atoms become equally probable, replacing Ge in the crystal lattice sites of the $(GaAs)_{1-x}(Ge_2)_x$ solid solution. In which the appearance of Ga and As atoms becomes equally probable, replacing Ge in the crystal lattice nodes of the solid solution. This allows the formation of a solid solution and the ordering of the crystal structure at different chemical compositions. This phenomenon was also observed in [13] during preparing multilayer heteroepitaxial solid solutions $(Ge_2)_x(GaAs)_{1-x}$ by pyrolytic synthesis.

It should be noted that among the many known methods for producing heterostructures, low-temperature liquid phase epitaxy (LPE) is one of the most important growth methods for new generations of optoelectronic devices. Competing methods, for example, chemical vapor deposition, are much more complex, although they involve quite subtle variation of film growth parameters [9,10,14]. According to [15], the LPE method makes it possible to obtain multilayer AlGaAs/GaAs structures with sharp heterointerfaces. In addition, it was shown in [16, 17] that growing GaAs epitaxial layers from a Ga–Bi–GaAs solution-melt on GaAs (100) substrates leads to the production of films with higher

*Corresponding author E-mail: dona23042014@gmail.com

structural perfection compared to epitaxial layers grown using as a Ga-based solvent. In this regard, the authors of [18] have already taken into account the solvent role, based on the state diagrams of the components in the system. Germanium-alloyed GaAs layers were grown from Ga-Bi solvents of various chemical compositions (from pure Ga to pure Bi) on GaAs (100) and GaAs (111) substrates. It was found that the main factor determining the interstition of Ge into the GaAs lattice during growth is the change in the concentrations of Ga and As in the liquid phase.

Thus, despite a significant amount of research devoted to the growth of semiconductor single-crystal epitaxial films, there has been no description in the literature of the multilayer structures production in a single technological cycle. In this regard, the purpose of this work is the physical interpretation of the processes occurring during the growth of heterostructures in a single cycle, as well as the production of such structures and the study of their electrical properties.

2. Materials and Methods

To grow the GaAs-Ge-$(Ge_2)_{1-x}(GaAs)_x$ heterostructure, we used a vertical quartz reactor with horizontally positioned substrates on an EPOS-type setup. The epitaxial layer was grown from a small volume of tin melt solution, limited by two substrates in an atmosphere of hydrogen purified by palladium, which made it possible to minimize the amount of melt solution consumed. First, a vacuum was created in the reactor to a residual pressure of 10^{-2} Pa, then purified hydrogen was passed through the reactor for 30 min, and then the heating process began. When the temperature reached the required value, the system switched to automatic mode. Homogenization of the melt solution was performed for 40-50 min. Then the substrates on the graphite holder were brought into contact with the melt solution and after filling the gaps between the substrates with the melt solution, they were raised 1 cm above the solution level. The growth of the epitaxial layers was stopped at the required moment by draining the melt solution from the substrates using a centrifuge. The growth was performed in a hydrogen atmosphere during the process. The composition of the melt solution consisting of Ge-Ga-As-Sn was determined from the phase diagram of the binary alloy Sn-Ge, Sn-GaAs [19–21].

Chemically pure (99.999%) GaAs (100) single crystal plates with a diameter of 20 and 40 mm and a thickness of 350 - 400 microns were used as a substrate. To obtain a specific melt solution based on a bismuth solvent, germanium and gallium arsenide powders were used.

Growing continuous multilayer solid solutions GaAs-Ge-$(Ge_2)_{1-x}(GaAs)_x$ in a single technological cycle was produced from a Bi-GaAs-Ge solution-melt in the temperature range 1023 K - 773 K. The distance between the substrates varied within 0.6 mm - 1.5 mm. The cooling rate was 0.5 -1.5 K/min.

Structural-phase studies were carried out on high-resolution diffractometers D2 PHASER/Bruker (GID and GONIO modes using HR-XRD, Panalytical/Empyrean). The study of the morphology and chemical content of the surface of the grown films was carried out using scanning electron microscopy (SEM EVO MA 10 (Zeiss) and atomic force microscopy (AFM).

Specific resistance, mobility and concentration of the main charge carriers were determined using an HMS-7000 (Hall effect measurement system). The spectral characteristics of the samples were measured using a monochromator with a slit diameter of 0.2 mm.

3. Results and discussion

In order to obtain high-quality semiconductor solid solutions with high physical and chemical properties on an industrial scale, it is necessary to develop theoretical prerequisites for their creation in order to optimize this process and reduce material costs. This is due to the physical parameters of the atoms involved in the formation of solid solutions. The statistical method proposed by Thomas and Fermi is used to determine the main features of the electron distribution and the electrostatic field in complex atoms. This makes it possible to predict in advance the creation of promising two-, three- and more-component semiconductor solid solutions before the experimental stage of scientific research.

Based on the fact that GaAs and Ge have isostructural lattices with similar parameter values (a_{GaAs} = 5.653 Å, a_{Ge} = 5.658 Å) and slightly different thermal expansion coefficients (α_{GaAs} = 5.0×10^{-6} K^{-1} and α_{Ge} = 5.7×10^{-6} K^{-1}), there is every reason to believe that a solid solution consisting of these components can have a high-quality crystalline structure, and its spectral viability may cover areas of germanium and gallium arsenide fundamental absorption.

The possibility of forming such a solid solution was estimated theoretically based on the general atomic moment (m*) calculation using the Thomas-Fermi formula for the multielectron atoms potential [22, 23]:

$$m^* = \frac{e\times Z}{r} \times \Phi\left(\frac{rZ^{\frac{1}{3}}}{0{,}8853 \times \frac{\hbar^2}{\mu e^2}}\right) \quad (1)$$

where e, μ - the charge and mass of the electron, Z and r - the serial number and radius of the atom, respectively, $\hbar$ - Planck's constant, $\Phi(x)$ - a function that is a solution to the Thomas-Fermi equation.

The generalized moments of atomic pairs calculated using this formula had the following values: for GaAs m^*=1.40×10^{-9} C/m, for Ge m^*= 1.34×10^{-9} C/m. As we can see, the difference between the generalized moments does not exceed 4.3%. This indicates a high probability of the $(Ge_2)_{1-x}(GaAs)_x$ type substitutional solid solution formation.

It should be noted that it is important to maintain thermodynamic equilibrium in the solution-melt system, i.e. the necessity of the components complete solubility at certain temperatures. In addition, it is important to take into account the influence of components mutual solubility in the melt solution. Crystallization of epitaxial layers on the substrate surface begins only when the melt solution is saturated with the required component at a certain temperature (the temperature at which crystallization begins) [24]. During the growth process, the surface of each new epitaxial layer serves as the basis (substrate) for the subsequent layer. Thus, a gradual change in the chemical composition along the growth direction (along the film thickness) leads to a smoothing of the difference between the crystal lattice parameters and thermal expansion coefficients in the substrate-film system. This helps to reduce the dislocation density, starting from the substrate-film boundary and continuing along the growth direction to the very surface of the grown film [25,26]. Therefore, to obtain predetermined cascade structures in a multicomponent system in the process of liquid phase epitaxy, taking into account the combination of saturation with different components, it is possible to control the chemical composition of the solid solution and grow multilayer materials. Epitaxial films GaAs-Ge-$(Ge_2)_{1-x}(GaAs)_x$ $(0\leq x\leq 1)$ just one of these materials, which are multilayer heterostructures grown in a single technological growth mode from a solution-melt. The film thickness ranged from 15 μm to 45 μm depending on the temperature of the beginning and end of crystallization.

Using the SEM method, the formation process of the $(Ge_2)_{1-x}(GaAs)_x$ solid solution, the chemical elements distribution over the surface of the growing film and the features of its morphology were studied (Fig. 1(a-f)). It was taken into account that any surface of a solid has a certain roughness, as a result of which the surface energy is distributed unevenly and affects the growth process.

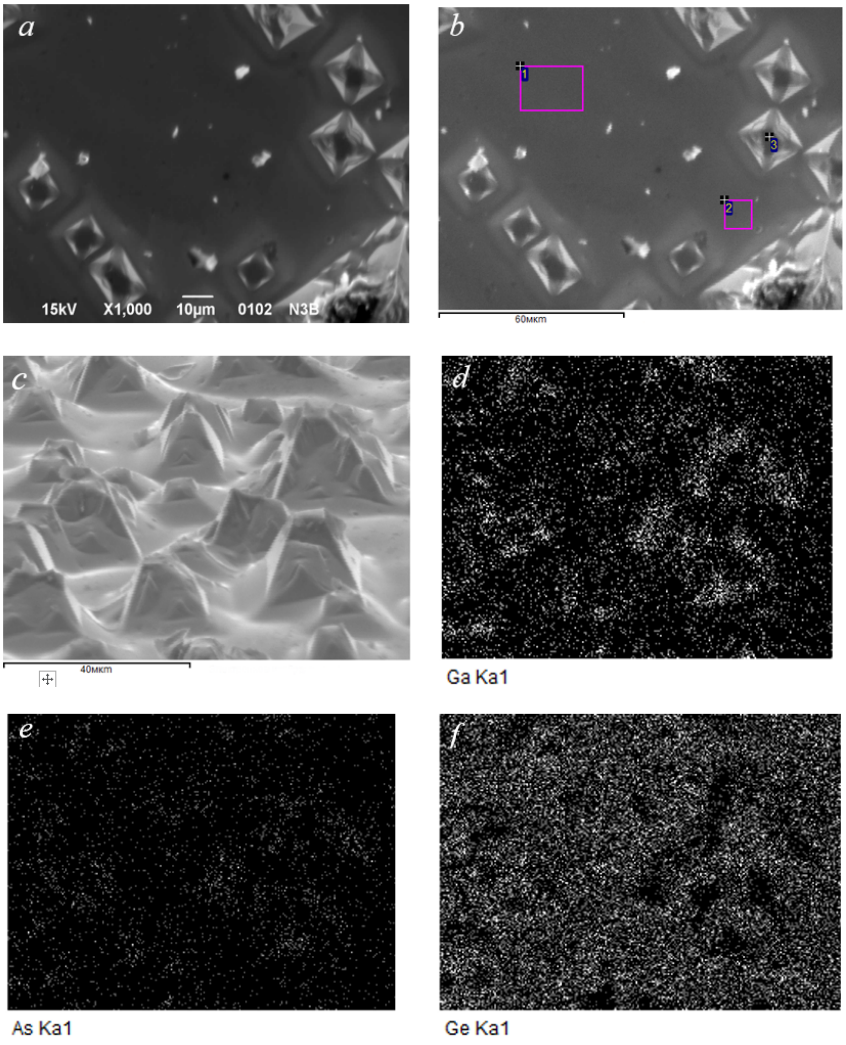

Fig. 1: The beginning of crystallization of the solid solution $(Ge_2)_{1-x}(GaAs)_x$ on the surface of the Ge buffer layer grown on the GaAs (100) substrate (a); distribution of the components Ga, As, Ge on the film surface (b), general view of the film surface at the initial stages of its growth on the buffer layer (c); Ga (d), As (e) and Ge (f) elemental maps of the film surface.

To determine the chemical composition and its change along the growth direction in the film, the growth process was

periodically interrupted until its final completion. That is, during the film growth in some processes, without finishing the growth process, the formation of epitaxial layers from the solution-melt was interrupted and studied. The state of the intermediate growth of the film was studied. This made it possible to determine the chemical composition and surface quality of the grown layer (Table 1).

Table 1: Chemical composition of surface areas of the grown GaAs-Ge-$(Ge_2)_{1-x}(GaAs)_x$ structure (Fig. 1, b)

Plot number	Ga at. %	at. % σ	Ge, at. %	at. % σ	As, at. %	at. % σ
1	0.60	0.12	98.73	0.43	0.67	0.12
2	1.20	0.17	97.37	0.51	1.43	0.18
3	27.81	0.33	34.35	0.37	37.84	0.38

The conducted studies showed that at the beginning of the process, the growth of an epitaxial GaAs layer began on the substrate, the orientation of which coincided with the (100) substrate orientation. As the film thickness increased, the Ge content in the growth direction increased, while the GaAs content decreased (Table 1). In the experimental episode shown in Fig. 1b, on the film surface, consisting almost entirely of germanium and already acting as a buffer layer, nuclei of the solid solution $(Ge_2)_{1-x}(GaAs)_x$, shaped like quadrangular pyramids, were formed, also repeating the substrate orientation (Fig. 1c). Elemental maps of the film surface showed the presence of elements Ga, As, and Ge in the composition of the solid solution (Fig. 1d-f). In this case, the distribution of components was uniform, and inclusions of other phases were absent.

Consider the physical reasons for the formation sequence of the heterostructure under study.

In this case, at a certain temperature (the beginning of crystallization), the melt solution will be “ready to grow” on the substrate surface due to its saturation with gallium arsenide. During program cooling at a certain rate, due to a decrease in the temperature of the system, epitaxial GaAs layers begin to crystallize on the substrate, repeating its orientation. In this case, there is a gradual decrease in the concentration of the GaAs component in the melt solution and an increase in the Ge concentration (according to the state diagrams for specific temperatures), which naturally leads to a decrease in the GaAs component and an increase in Ge in the growing epitaxial layers. Thus, as the temperature decreases, the melt solution is gradually saturated with germanium, which leads to a change in the film chemical composition along the direction of its growth. As a result, a buffer epitaxial layer is formed with a surface containing almost only germanium. Therefore, at the next stage, due to this, the epitaxial Ge layer grew. Then the total film thickness was 32.3 μm.

A further decrease in temperature during growth leads to the opposite effect: the amount of Ge in the growing layer decreases, and the amount of GaAs increases, in other words, the growth of the $(Ge_2)_{1-x}(GaAs)_x$ heterostructure film begins again with a gradient change in composition along the growth direction. The process ends with the formation of a GaAs surface epitaxial layer, practically free of germanium (Fig.2, a,b). Each subsequent epitaxial layer $(Ge_2)_{1-x}(GaAs)_x$ had a crystallographic orientation of the previously formed structures. It is worth noting that the orientation of the single-crystal GaAs substrate (100) is the most favorable for the described growth process.

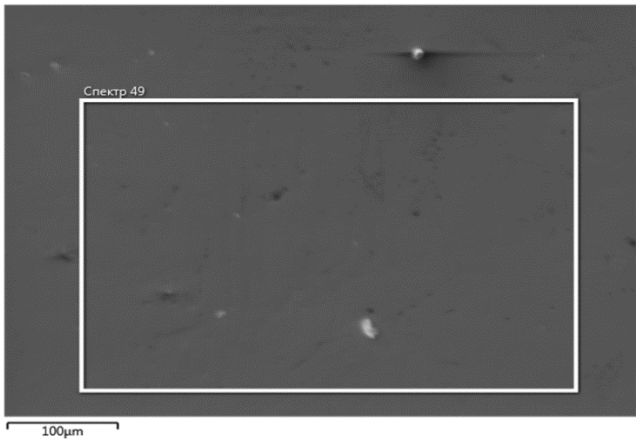

(a)

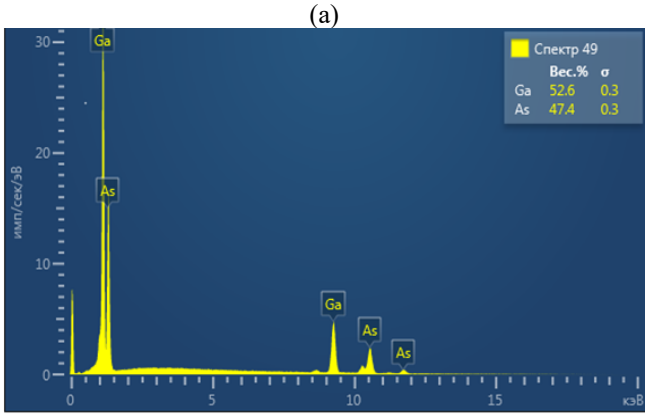

(b)

Fig. 2: Scanning electron microscope images: the final surface of the heterostructured epitaxial film GaAs-Ge-$(Ge_2)_{1-x}(GaAs)_x$ (x = 1), grown in a single technological cycle on a GaAs (100) substrate (a) and the energy spectrum of this surface (b)

Such alternation of layers with variable chemical compositions makes it possible at the end of the technological process to obtain a three-layer sandwich-type heterostructure grown on a single-crystal GaAs substrate, which is confirmed by a change in the chemical composition along the grown films thickness (Fig. 3). The measurement error is 0.3% (shown in the upper corner of Figure 2b).

Due to the sequential alternation of the indicated processes, which occurred naturally, it was possible to obtain the GaAs-Ge-$(Ge_2)_{1-x}(GaAs)_x$ structure in a single technological cycle of crystallization from the liquid phase.

In our opinion, it is very important that taking into account the change in the saturation of the solution-melt with GaAs and Ge components at a certain temperature, as well as the cooling rates of the system during the growth process, makes it possible to change the chemical elements distribution along the growth direction, which makes it possible to purposefully control the elementary layers chemical composition, thereby influencing the electrophysical properties of the final product.

It should be noted that the highest quality heterostructure GaAs-Ge-$(Ge_2)_{1-x}(GaAs)_x$ ($0 \leq x \leq 1$) was obtained at a crystallization onset temperature of 1023 K, solution-melt cooling rate 1 K/min. The gap between the substrates did not exceed 1.2 mm, which is consistent with [27]. The dislocation density on the film surface was 2×10^4 cm^{-2}.

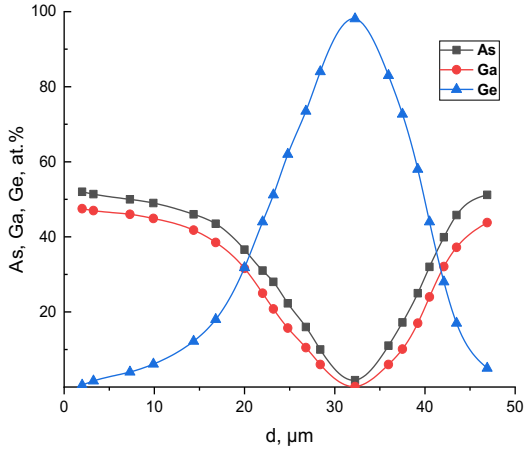

Fig. 3: Dependence of the chemical composition of the solid solution GaAs-Ge-$(Ge_2)_{1-x}(GaAs)_x$, grown from a bismuth solution-melt along the growth direction (by the thickness *d* of the film) studied using the SEM method.

Further studies were devoted to the resulting epitaxial films quality. The morphology of the $(Ge_2)_{1-x}(GaAs)_x$ film surface was studied using CoreAFM. The surface roughness varied within 1.66 - 1.18 nm (rms roughness value 1.455 nm) (Fig. 4). According to [28], the resulting films surfaces can be considered quite smooth. Since the epitaxial layers surface did not contain any noticeable faceting, it can be considered as a single-crystal film with a high-quality surface. Thus, good surface morphology of each growing epitaxial layer, as well as ordered alternation of layers, makes it possible to obtain crystalline perfect films with varying chemical compositions, which is the basis for obtaining multilayer structures in a single technological cycle.

According to XRD studies, reflections from planes (200), (400) and (600) were observed in the diffraction patterns, which indicated the single-crystal nature of the surface layers of the grown film (Fig. 5). It is necessary to note a certain shift of the diffraction maxima to the region of larger Bragg angles compared to reflections from the GaAs substrate lattice. Precision measurement of the lattice parameter $a_\perp$ of the obtained solid solution indicated its decrease ($a_{(Ge2)1-x(GaAs)x}$=5.6516±0.0004 Å), compared to the lattice parameters of both germanium (a_{Ge} = 5.6581±0.0004 Å) and gallium arsenide (a_{GaAs}=5.6532±0.0004 Å), which is not consistent with Vegard's rule.

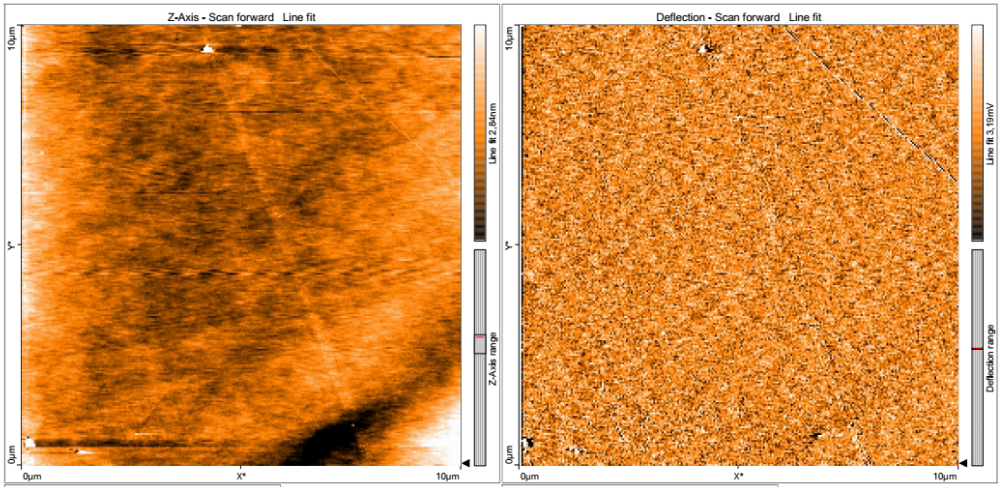

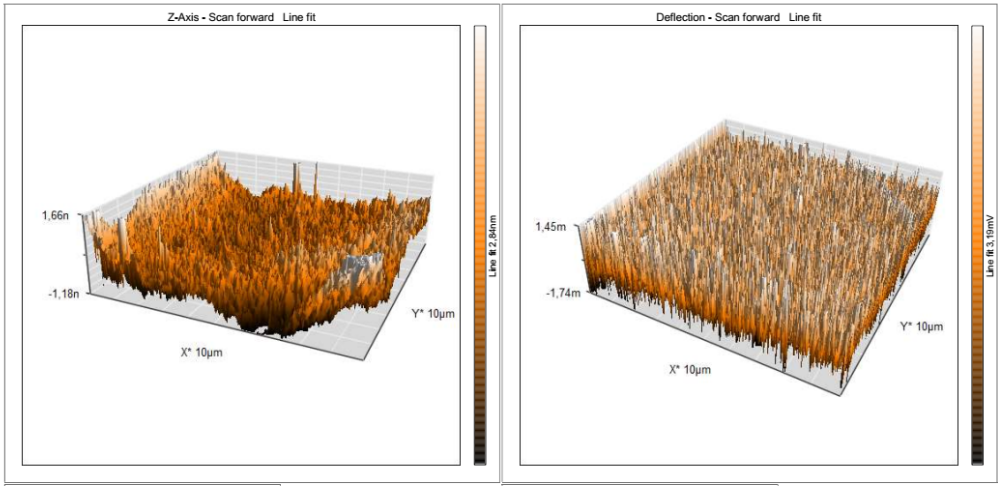

Fig. 4: 2D and 3D AFM images of the surface of a $(Ge_2)_{1-x}(GaAs)_x$ heterostructure epitaxial film grown on a GaAs substrate

In our opinion, the reason for such a decrease in the lattice parameter could be tensile stresses arising in the plane of the film surface. Their occurrence is due to the fact that the lattice parameter of germanium is greater than the lattice parameter of gallium arsenide. Then the lattice parameter of the grown film in the plane parallel to the substrate ($a_{\parallel}$) should exceed the tabulated value for GaAs. In this case, the unit cell will not be cubic, but tetragonal. This can explain the discrepancy between the measured lattice parameter $a_{\perp}$ and Vegard's rule.

More accurate information on this can be obtained by numerically modeling reciprocal space maps, which is a separate task [29,30].

Finally, some electrophysical properties of the resulting films were investigated. The specific resistance, Hall mobility and charge carrier concentration at a temperature of 300 K were determined: ρ = 0.5-14 Ω×cm, μ_p = 100 $cm^2/V\times s$, $n_p = 1.25\times10^{18}$ cm^{-3}. The films had an acceptor type of conductivity.

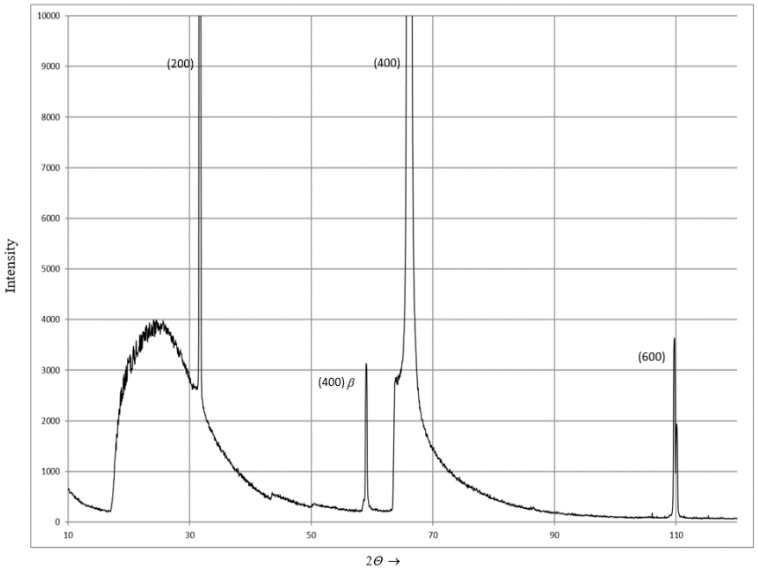

Fig. 5: XRD patterns from the epitaxial layer surface (Cu-K_α-radiation)

Growing a solid solution synthesized from several semiconductor components integrates the characteristics of each of them. In our case, the photosensitivity range of Ge and GaAs. That is, the specific optical properties of the $(Ge_2)_{1-x}(GaAs)_x$ solid solution and *n*GaAs-*p*Ge-*p*$(Ge_2)_{1-x}(GaAs)_x$ structures based on them make it possible to use them as a material for photodetectors operating in a relatively wide spectral region, overcoming the limitations of infrared photonics [31]. The photosensitivity of the *n*GaAs-*p*Ge-*p*$(Ge_2)_{1-x}(GaAs)_x$ structure was measured in photodiode mode at a temperature of 300 K and covered the spectral range from 0.65 eV to 2.0 eV. In this case, two maxima of photosensitivity were observed at energy values of the incident spectral quanta of 0.7 eV and 1.43 eV (Fig. 6).

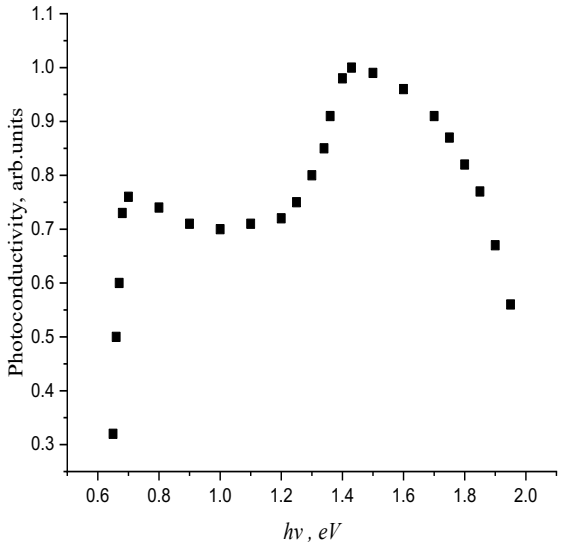

Fig. 6: Photosensitivity of the *n*GaAs-*p*Ge-*p*$(Ge_2)_{1-x}(GaAs)_x$ structure in the photodiode mode at a temperature of 300 K

The first maximum of photosensitivity (0.7 eV) is probably associated with an increase in the concentration of nonequilibrium charge carriers under the influence of incident quanta on the nGaAs-pGe (substrate-film) transition. The presence of the second photosensitivity maximum (1.43 eV) can be explained by the features of the *n*GaAs-*p*Ge-*p*$(Ge_2)_{1-x}(GaAs)_x$ structure. The band gap in the $(Ge_2)_{1-x}(GaAs)_x$ layer is larger than in Ge, so it transmits incident quanta with energies exceeding 0.7 eV. And then the generated charge carriers reaching the heterojunction can participate in current flow. Epitaxial layers with a significant germanium content (up to almost pure Ge) in the $(Ge_2)_{1-x}(GaAs)_x$ solid solution, due to their graded band-gap nature, can be considered as a transition accelerating layer in the *n*GaAs-*p*Ge-*p*$(Ge_2)_{1-x}(GaAs)_x$ structure during the movement of charge carriers. This conclusion follows from the fact that, depending on the composition of the $(Ge_2)_{1-x}(GaAs)_x$ ($0 \le x \le 1$) solid solution, the band gap changes along the growth direction (Fig.7).

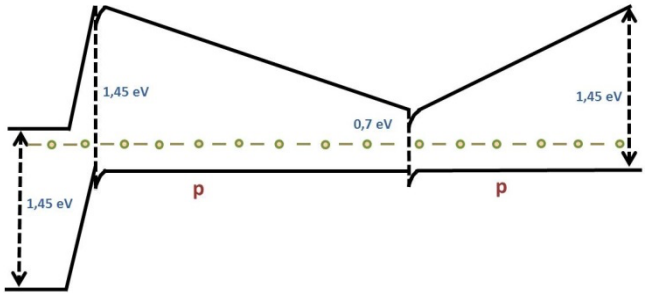

Fig. 7: Band diagram of the *n*GaAs-*p*Ge-*p*$(Ge_2)_{1-x}(GaAs)_x$ structure

This leads to the creation of an electric field intensity in the film, directed from the substrate-film boundary to its surface.

4. Summary

1. A technology has been developed for growing GaAs-Ge-GaAs multilayer structures from a limited bismuth solution-melt in a single technological cycle, which, in terms of energy costs and process simplification, is promising for creating epitaxial films with a wide range of photosensitivity.
2. Graded-gap epitaxial layers $(Ge_2)_{1-x}(GaAs)_x$ with a composition gradiently enriched up to pure Ge, located between the GaAs substrate and the film surface, serve as an accelerating buffer layer for charge carriers in the nGaAs-pGe-p$(Ge_2)_{1-x}(GaAs)_x$ structure.
3. The presence of two maxima on the photosensitivity curve measured in the photodiode mode is associated with the heterostructural structure peculiarities of the epitaxial films grown in a single cycle.

References

[1] X. Lu, Y. Minami, T. Kitada Sublattice reversal in GaAs/Ge/GaAs and AlAs/Ge/AlAs heterostructures grown on (113)A and (113)B GaAs substrates. *Journal of Crystal Growth*. 2019, Vol. 512, P.74-77.

[2] S. Koh, T.Kondo, Y.Shiraki, R.Ito. GaAs/Ge/GaAs sublattice reversal epitaxy and its application to nonlinear optical devices. *Journal of Crystal Growth*. 2001, 227-228, P.183-192.

[3] Mantu K. Hudait; Yan Zhu; Nikhil Jain; Siddharth Vijayaraghavan; Avijit Saha; Travis Merritt; Giti A. Khodaparast. In situ grown Ge in an arsenic-free environment for GaAs/Ge/GaAs heterostructures on off-oriented (100) GaAs substrates using molecular beam epitaxy. *J. Vac. Sci. Technol*. B 30, 051205 (2012). https://doi.org/10.1116/1.4742904.

[4] Lu X., Kumagai, N., Minami, Y., Kitada, T. Sublattice reversal in GaAs/Ge/GaAs heterostructures grown on (113)B GaAs substrates. *Applied Physics Express*. V.11, Iss.1, 2018, 015501. DOI: 10.7567/APEX.11.015501.

[5] M.K. Hudait, Y.Zhu, N. Jain, J.L.Hunter. Structural, morphological, and band alignment properties of GaAs/Ge/GaAs heterostructures on (100), (110), and (111) GaAs substrates. *Journal of Vacuum Science & Technology B, Nanotechnology and Microelectronics: Materials, Processing, Measurement, and Phenomena*, 31(1), 011206. 2013. http://dx.doi.org/10.1116/1.4770070.

[6] X. Lu, Y. Minami, T. Kitada. Sublattice reversal in GaAs/Ge/GaAs and AlAs/Ge/AlAs heterostructures grown on (1 1 3)A and (1 1 3)B GaAs substrates. Journal of Crystal Growth. 2019. V.512, 2019, P.74-77. DOI:10.1016/J.JCRYSGRO.2019.02.010.ID: 104419805

[7] D. Zhang, W. Lou, M. Miao, S. Zhang, K. Chang. Interface-Induced Topological Insulator Transition in GaAs/Ge/GaAs Quantum Wells PRL 111, 156402 (2013) *Phys.Rev.Lett*. DOI: 10.1103/PhysRevLett.111.156402.

[8] C.Gunder, F.Maia de Oliveira, E.Wangila, H.Stanchu, M.Zamani-Alavijeh, S.Ojo, S.Acharya, A.Said, C.Li, Y.I.Mazur, S.Yu, G.J.Salamo. The growth of Ge and direct bandgap $Ge_{1-x}Sn_x$ on GaAs (001) by molecular beam epitaxy RSC Advances.V.14, Iss.2, 2024, P.1250-1257. https://doi.org/10.1039/d3ra06774b

[9] S.Giraud, T.Duffar, E.Pihan, A.Fave. Kinetics modeling and growth of Si layers by Liquid Phase Epitaxy Driven by Solvent Evaporation (LPESE). Journal of Crystal Growth.Vol.432, 2015, P.8391.https://doi.org/10.1016/j.jcrysgro.2015.08.002

[10] B.E.Tew, M.R.Lewis, C.Y.Hsu, Ch.Ni, J.O.Zide. Growth of ErAs:GaAs nanocomposite by liquid phase epitaxy. Journal of Crystal Growth. Vol.518, 2019, P.34-38. https://doi.org/10.1016/j.jcrysgro.2019.04.025

[11] B.Salazar-Hernández, M.A.Vidal, M.E.Constantino, H.Navarro-Contreras, R.Asomoza, A.Merkulov. Structural study of metastable $(GaAs)_{1-X}(Ge_2)_X$ thin films grown by RF magnetron sputtering. *Journal of Crystal Growth*.V.197, Iss.4, 1999, P.783-788. https://doi.org/10.1016/S0022-0248(98)00958-0.

[12] A.G.Rodríguez, H.Navarro-Contreras, M.A.Vidal. Long-range order–disorder transition in $(GaAs)_{1-x}(Ge_2)_x$ grown on GaAs(001) and GaAs(111). *Microelectronics Journal*. V.31, Iss.6, 2000, P.439-441. https://doi.org/10.1016/S0026-2692(00)00008-2

[13] Zh.I. Alferov et al. Preparation and study of metastable continuous solid solutions in the Ge-GaAs system. *Physics and technics of semiconductors* V.15, N5, P.831-839.

[14] F.Starecki, W.Bolaños, G.Brasse, A.Benayad, M.Morales, J.Doualan, A.Braud, R.Moncorgé, P.Camy. Rare earth doped LiYF4 single crystalline films grown by liquid phase epitaxy for the fabrication of planar waveguide lasers. Journal of Crystal Growth.Vol.401,2014, P.537-541. https://doi.org/10.1016/j.jcrysgro.2014.01.039

[15] M.Milanova, V.Khvostikov. Growth and doping of GaAs and AlGaAs layers by low-temperature liquid-phase epitaxy. *Journal of Crystal Growth*. V.219, Iss.3, 2000, P.193-198 https://doi.org/10.1016/S0022-0248(00)00624-2.

[16] K.Jeganathan, S.Saravanan, P.Ramasamy, J.Kumar. Effect of bismuth on liquid-phase epitaxy (LPE) grown GaAs layer using Ga–As–Bi melt. *Journal of Crystal Growth*.V.200, Iss.3–4, 1999, P.341-347. https://doi.org/10.1016/S0022-0248(99)00075-5.

[17] M.Milanova, P.Terziyska. Low-temperature liquid-phase epitaxy growth from Ga–As–Bi solution. *Thin Solid Films*. V.500, Iss.1–2, 2006, P.15-18 https://doi.org/10.1016/j.tsf.2005.10.049.

[18] N.A.Yakusheva, V.G. Pogadaev. Amphoteric behaviour of germanium during liquid phase epitaxy of GaAs from bimuth-gallium melt. *Journal of Crystal Growth*. V.123, Iss.3–4, 1992, P.479-486. https://doi.org/10.1016/0022-0248(92)90609-M

[19] G.B.Stringfellow, P.E.Green. A quasi-chemical equilibrium calculation of Ge-Si-Sn and Ge-Si-Pb ternary phase diagrams.-«J.Electrochem. Soc.», 1970, v.117,N8, p.1075.

[20] Rubinstein M. Solubilities of gallium arsenide in metallic solvents.-«J.Electrochem. Soc.», 1966, v.113,N7, p.752.

[21] McAlister, A.J., Kahan, D.J. The Al−Sn (Aluminum-Tin) System. Bulletin of Alloy Phase Diagrams 4, 410–414 (1983). https://doi.org/10.1007/BF02868095

[22] Morgan III, J. (2023). Thomas-Fermi and Other Density-Functional Theories. *Springer Handbook of Atomic, Molecular and Optical Physics*. New York, NY. Chapter pp.295–306. https://doi.org/10.1007/978-3-030-73893-8_21

[23] S.Rekhviashvili, A.Sokurov. Fractal generalization of Thomas–Fermi model. *The Physics of Metals and Metallography*. (2016), V.117, N5, p.423-425. DOI: 10.1134/S0031918X1605015X.

[24] Saidov A. S. et al. Obtaining $Si\text{-}Si_{1-x}Ge_x\text{-}(Si_{1-x}Ge_x)_{1-z}(Al_{1-y}Ga_yAs)_z\text{-}Si_{1-x}Ge_x\text{-}(Si_{1-x}Ge_x)_{1-z}(Al_{1-y}Ga_yAs)z$ Structures from a Tin Solution-Melt in a Single Technological Cycle //*Acta Physica Polonica*, A. – 2022. – Vol. 142. – №. 2.

[25] I. E. Maronchuk, S. R. Sorokolet, I. E. Maronchuk. Features of the deformation of Ge-GaAs heterostructures under loads // *Technical Physics Letters*. – 1998, – Vol. 24, – No. 6, – pp. 475-476.

[26] Saidov A. S., Razzokov A. S. Growth and Morphological Study of Graded-Gap Si– $Si_{1-x}Ge_x$ – GaAs Structures //*Crystallography Reports*. – 2022. – Vol. 67. – №. 2. – С. 301-305.

[27] A.Sh.Razzokov. A.S.Saidov, V.V.Girzhon, O.V.Smolyakov. Features of growing Si-and Si1–xGex -single-crystal films from solution-melt based on tin //*Journal of Physical Studies*. – 2022. – Vol. 26. – №. 4. – P. 4601-1-4601-5.

[28] J.Yu and Y. Namba. Atomic surface roughness. *Appl. Phys.* V.73, N24, pp.3607-3609 (1998). https://doi.org/10.1063/1.122839

[29] D.Zhou, B.F.Usher. Deviation of the AlGaAs lattice constant from Vegard's law. J. Phys. D: Appl. Phys.

34 (2001) 1461–1465)

[30] P.V.Seredin, A.V.Glotov, E.P.Domashevskaya, I.N. Arsentyev, D.A.Vinokurov, A.L.Stankevich, I.S. Tarasov. Relaxation of crystal lattice parameters and structural ordering in epitaxial solid solutions InxGa1−xAs. Semiconductors, 2010, V.44, Iss.8, P.1140-1146).

[31] Zhen Hu et al. Terahertz Nonlinear Hall Rectifiers Based on Spin-Polarized Topological Electronic States in 1T-CoTe2. Advanced Materials. 35.10(2023), 2209557. DOI: 10.1002/adma.202209557